Coupled chaotic chemical oscillators

Milos Dolnik and Irving R. Epstein
Department of Chemistry and Volen Center for Complex Systems, Brandeis University, Waltham, Massachusetts 02254-9110
(Received 8 April 1996; revised manuscript received 10 June 1996)

We present a model study of two mass-coupled reactors containing the Belousov-Zhabotinsky reaction under chaotic conditions. The critical coupling strength is estimated for symmetry breaking when two identical low flow rate chaotic modes are coupled. Our results confirm that the critical coupling strength is directly proportional to the maximum Lyapunov exponent of the uncoupled system. The constant of proportionality is found to be somewhat larger than the theoretical value. Direct integration reveals a rich structure of dynamical behavior when the coupling strength and the flow rate in one cell are varied. Our simulations reveal domains of oscillator death, in which a stable steady state coexists with limit cycle oscillations. We introduce a simple model for predicting the dynamics of the coupled system from the dynamical behavior of the uncoupled subsystems and the dependence on the coupling strength of the Hopf bifurcation of the coupled system. The model gives good estimates of the dynamical behavior of two coupled oscillators with a small difference in one parameter at intermediate and high coupling strengths. [S1063-651X(96)01210-X]

PACS number(s): 05.45.+b

I. INTRODUCTION

Coupled oscillatory, bistable and excitable chemical systems have been a subject of intense experimental [1–11] and numerical [12–16] investigation for more than two decades, and coupled chaotic systems have been studied analytically, numerically, and experimentally in several fields for almost as long [17–30]. Only quite recently, however, has the study of coupled chaotic oscillators been extended to chemical systems [31,32]. The nature of the coupling is a distinctive feature of any coupled system. Mass exchange is the most commonly employed form of coupling in chemical oscillators [1–4,6–11]. Another type of coupling has been accomplished electrically, via the connection of electrodes [5] in two continuous flow stirred tank reactors (CSTR's).

The Belousov-Zhabotinsky (BZ) reaction [33] is the most studied oscillating chemical reaction. Although deterministic chaos was found in the BZ reaction over twenty years ago [34,35], the first chemically realistic model of chaos in the BZ system was suggested by Györgyi and Field only within the past few years [36,37]. Aperiodic oscillations are found both at low and at high flow rates in the BZ flow system. While there was no dispute about the presence of deterministic chaos at low flow rates, the origin of aperiodicity at high flow rates was a subject of controversy in the early 1990s. Schneider and Münster [38] attributed the aperiodic oscillations to statistical noise, while Györgyi *et al.* [39] took the reproducibility of complex dynamics as an indication of deterministic chaos. In support of this latter contention, Györgyi and others have shown that a four-variable model of the BZ reaction qualitatively reproduces the complex periodic and chaotic behavior, including the aperiodic oscillations at a high flow rate.

Hauser and Schneider [32] have studied the coupling of identical chaotic modes in the BZ reaction at low flow rate. They find that at high coupling strengths the coupled chaotic states become synchronized, while at low coupling strengths the chaotic states are asynchronous with close to zero correlation. At intermediate coupling, where a symmetry-breaking transition occurs, they directly evaluate the largest Lyapunov exponent of the single system from the coupling strength.

In this paper we pursue a more global investigation of coupled chaotic chemical oscillators at both low and high flow rates. We investigate a model of the BZ reaction in the chaotic mode in a system of two reactors either with identical or with different parameters. In the system with identical parameters, we study the symmetry-breaking transition at intermediate coupling strengths and determine the critical values of coupling for several chaotic modes. In studying two oscillatory systems described by the same set of rate equations but with different values of one system parameter, the flow rate, we look for the emergence of oscillator death [40]. We propose a simple model for predicting the dynamics of the coupled oscillators from the dynamical properties of the uncoupled subsystems and the dependence of the Hopf bifurcation of the coupled system on the coupling strength.

II. PRELIMINARY CONSIDERATIONS

A. Mathematical model

To model the coupled chemical oscillators we employ a model suggested by Györgyi and Field [37] to describe chaos and other dynamical behavior in the BZ reaction

$$\mathrm{Br^-}+\mathrm{HBrO_2}+\mathrm{H^+}\rightarrow 2\mathrm{BrMA}$$

$$r_1=2.0\times 10^6[\mathrm{H^+}][\mathrm{Br^-}][\mathrm{HBrO_2}]$$

$$\mathrm{Br^-}+\mathrm{BrO_3^-}+2\mathrm{H^+}\rightarrow \mathrm{BrMA}+\mathrm{HBrO_2}$$

$$r_2=2.0[\mathrm{H^+}]^2[\mathrm{BrO_3^-}][\mathrm{Br^-}]$$

$$2\mathrm{HBrO_2}\rightarrow \mathrm{BrMA}\quad r_3=2\times 10^3[\mathrm{HBrO_2}]^2$$

$$0.5\mathrm{HBrO_2}+\mathrm{BrO_3^-}+\mathrm{H^+}\rightarrow \mathrm{HBrO_2}+\mathrm{Ce^{4+}}$$

$$r_4=6.2\times 10^4[\mathrm{H^+}]([\mathrm{Ce}]_{\mathrm{tot}}-[\mathrm{Ce^{4+}}])[\mathrm{BrO_2^-}]_{\mathrm{est}}$$

TABLE I. Constants in Eq. (1)—fixed concentrations.

$[H^+]$ (M)	0.26
$[BrO_3^-]$ (M)	0.1
$[Ce]_{tot}$ (M)	0.001
[MA] (M)	0.25

$$HBrO_2+Ce^{4+}\rightarrow 0.5HBrO_2 \quad r_5=7\times10^3[HBrO_2][Ce^{4+}]$$

$$Ce^{4+}+MA\rightarrow \quad r_6=0.3[MA][Ce^{4+}]$$

$$BrMA+Ce^{4+}\rightarrow Br^- \quad r_7=30[BrMA][Ce^{4+}]$$

$$BrMA\rightarrow Br^- \quad r_8=2.4\times10^4[BrMA][MA^{\cdot}]_{qss},$$

where

$$[MA^{\cdot}]_{qss}=\{-2.4\times10^4[BrMA]+((2.4\times10^4[BrMA])^2 +7.2\times10^9[MA][Ce^{4+}])^{0.5}\}/1.2\times10^{10},$$
$$[BrO_2^{\cdot}]_{est}=\{0.858[BrO_3^-][H^+][HBrO_2]/4.2\times10^7\}^{0.5}, \quad (1)$$

and

$$[Ce]_{tot}=[Ce^{4+}]+[Ce^{3+}].$$

The concentrations $[H^+]$, $[BrO_3^-]$, $[Ce]_{tot}$ and malonic acid [MA] are taken to be constant; their values are shown Table I. The mathematical model of reaction scheme (1) with these approximations in a single CSTR consists of four ordinary differential equations with variables $x_1\equiv[HBrO_2]$, $x_2\equiv[Br^-]$, $x_3\equiv[Ce^{4+}]$, $x_4\equiv[BrMA]$

$$\frac{dx_1}{dt}=-r_1+r_2-2r_3+0.5(r_4-r_5)+k_o(x_{o1}-x_1),$$
$$\frac{dx_2}{dt}=-r_1-r_2+r_7+r_8+k_o(x_{o2}-x_2),$$
$$\frac{dx_3}{dt}=r_4-r_5-r_6-r_7+k_o(x_{o3}-x_3), \quad (2)$$
$$\frac{dx_4}{dt}=2r_1+r_2+r_3-r_7-r_8+k_o(x_{o4}-x_4),$$

where k_o is the flow rate and x_{oi} are the inflow concentrations.

B. Single CSTR

The dynamics corresponding to reaction scheme (1) in a single CSTR include chaotic behavior at low and at high flow rates. The dynamical behavior is summarized in the bifurcation diagrams of Fig. 1, which display the extrema of the oscillations at low [Fig. 1(a)] and at high flow rates [Fig. 1(b)]. A periodic state is represented by a finite number of points at a given flow rate, while a continuous group of points signifies a chaotic state. The largest windows of periodic behavior are denoted as P_i, the largest chaotic domains are denoted as C.

We have calculated the full spectrum of Lyapunov exponents by the method of Wolf *et al.* [41] in order to confirm the presence of chaos and to distinguish true chaotic behavior from quasiperiodicity or periodic behavior with a high periodicity. The largest Lyapunov exponent is shown in the bottom frames of Figs. 1(a), 1(b). Positive values of the Lyapunov exponent indicate deterministic chaos, which occurs, as it does in the experiments, in relatively narrow windows of the flow rate parameter.

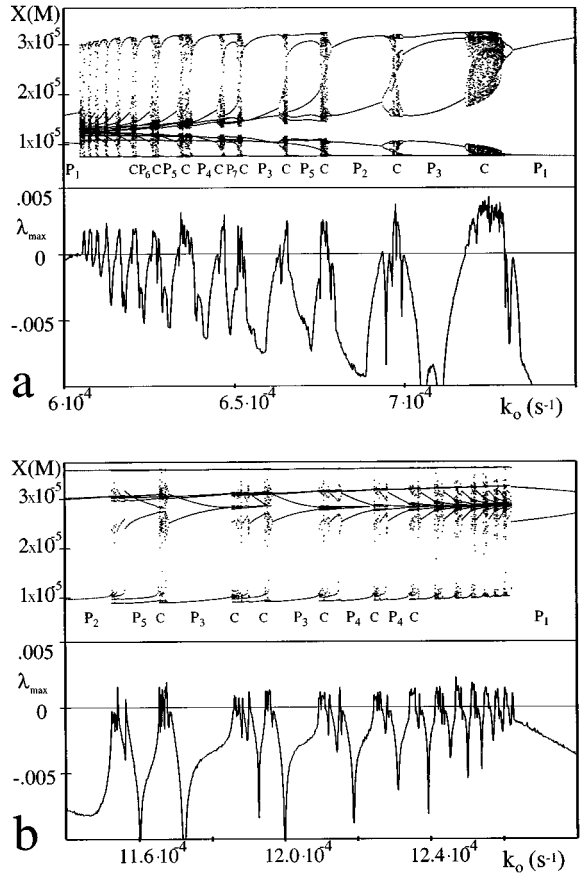

FIG. 1. One-parameter bifurcation diagrams and plots of the largest Lyapunov exponent for model (1) of the BZ reaction in a single CSTR at low (a) and high (b) flow rates. Points in bifurcation diagrams correspond to extrema values. Small numbers of points and negative values of λ_{max} correspond to periodic states, while many points and positive values of λ_{max} indicate chaos. The largest domains of chaos are denoted as C and the largest domains of periodic oscillation as P_i, where the subscript gives the periodicity.

There are two supercritical Hopf bifurcation points, which indicate the limiting values of the flow rate within which the single subsystem oscillates. These Hopf points are located at $k_o=5.859\,64\times10^{-4}$ s^{-1} and at $k_o=1.289\,883\times10^{-3}$ s^{-1}. We shall show later how the structure of alternating periodic and chaotic regions in the uncoupled subsystems can be used to predict the dynamics of coupled CSTRs.

C. Coupled CSTRs

The time evolution of a system of two well mixed reactors coupled by symmetric mass transfer (diffusionlike) coupling can be written in the following form:

$$\frac{dx_k^{(i)}}{dt}=R_k(x_1^{(i)},x_2^{(i)},\ldots,x_n^{(i)})+k_o^{(i)}(x_{ok}^{(i)}-x_k^{(i)})+k_c(x_k^{(j)}-x_k^{(i)}), \quad (3)$$

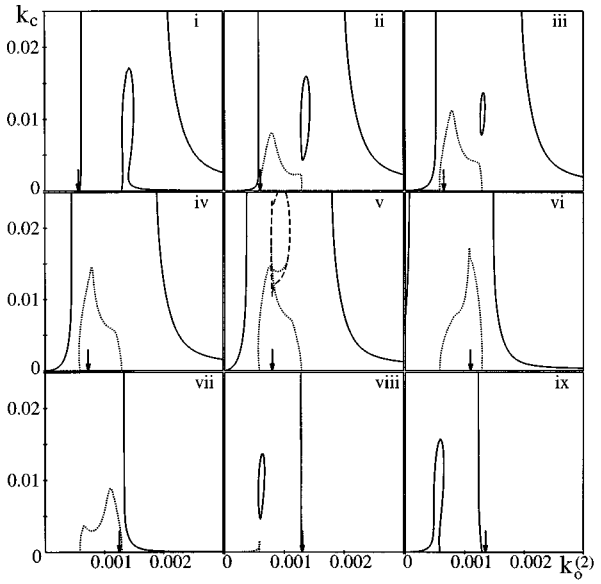

FIG. 2. Two-parameter bifurcation diagrams for model of two coupled oscillators. Solid curve is primary Hopf bifurcation; dotted curve is secondary Hopf bifurcation. Solid loop inside the oscillatory region is associated with oscillator death. Dashed curve is a saddle-node bifurcation line. Arrows indicate the fixed flow rate $k_o^{(1)}$ for each diagram (in s^{-1}): (i) 5.6×10^{-4}, (ii) 6.0×10^{-4}, (iii) 6.52×10^{-4}, (iv) 7.24×10^{-4}, (v) 8.0×10^{-4}, (vi) 1.1×10^{-3}, (vii) 1.25×10^{-3}, (viii) 1.3×10^{-3}, (ix) 1.35×10^{-3}.

where the superscripts $i,j=1,2$, $i\neq j$, identify the reactors; $x_1^{(i)}, x_2^{(i)},\ldots, x_k^{(i)},\ldots, x_n^{(i)}$ are the concentrations of the n chemical species in reactor i; R_k is the rate law for the kth reactant; $k_o^{(i)}$ is the flow rate into reactor i, $x_{ok}^{(i)}$ is the input concentration of reactant k in the inflow to reactor i; and k_c is the rate of mass exchange between the reactors.

For numerical analysis of the system we employ the CONT numerical bifurcation and continuation package [42]. The values of all parameters, except k_c, $k_o^{(1)}$ and $k_o^{(2)}$, are fixed (Table I) and equal in both cells.

III. RESULTS

A. Steady state analysis and oscillator death

In Fig. 2 we show the results of a two-parameter $(k_c-k_o^{(2)})$ bifurcation analysis for several fixed values of the flow rate $k_o^{(1)}$. The solid lines indicate a primary Hopf bifurcation, at which the real parts of two complex eigenvalues become zero while the real parts of all other eigenvalues are negative. On crossing the primary Hopf line, the number of eigenvalues associated with unstable manifolds changes from 0 to 2. The dotted lines denote a secondary Hopf bifurcation, at which two complex eigenvalues have zero real parts while the real parts of two other complex eigenvalues are positive. On crossing the secondary Hopf line, the number of eigenvalues associated with unstable manifolds changes from 2 to 4.

When $k_o^{(1)}\in(6.8\times10^{-4}\ s^{-1},\ 1.26\times10^{-3}\ s^{-1})$, there are only two primary Hopf lines, both of which are supercritical and thus indicate the domain of k_c and $k_o^{(2)}$ within which oscillatory behavior occurs. When $k_o^{(1)}<6.8\times10^{-4}\ s^{-1}$ or $k_o^{(1)}>1.26\times10^{-3}\ s^{-1}$, an additional primary Hopf line forms a loop inside the oscillatory region. The steady state solution is stable inside the loop and unstable outside. The Hopf bifurcation is subcritical along the loop, which implies that the stable steady state coexists with a stable limit cycle. Depending on the initial conditions, a trajectory will either reach the steady state or will traverse the limit cycle. Finite perturbation of the limit cycle can lead to cessation of oscillation, i.e., to oscillator death.

B. Synchronization of identical chaotic oscillators

One measure of the degree of synchronization of two oscillators is given by the correlation coefficient. For the ith species, we define the correlation coefficient C_i^{12} as

$$C_i^{12}=\frac{\Sigma_{j=1}^{N}(x_{i,j}^{(1)}-\langle x\rangle_i^{(1)})(x_{i,j}^{(2)}-\langle x\rangle_i^{(2)})}{[\Sigma_{j=1}^{N}(x_{i,j}^{(1)}-\langle x\rangle_i^{(1)})^2]^{1/2}[\Sigma_{j=1}^{N}(x_{i,j}^{(2)}-\langle x\rangle_i^{(2)})^2]^{1/2}}. \quad (4)$$

The subscript i designates the species, while the subscript j enumerates the N measurements that make up each time series. The superscript $(k)=(1)$ or (2) specifies the reactor, and the bracketed quantities $\langle x\rangle$ are averages over each time series.

Another measure of the similarity or difference between the time series in the two reactors is given by the average distance ΔX^{12}

$$\Delta X^{12}=\frac{1}{n}\sum_{i=1}^{n}\left[\sum_{j=1}^{N}(x_{i,j}^{(1)}-x_{i,j}^{(2)})^2\right]^{1/2}. \quad (5)$$

Hauser and Schneider [32] show that the correlation coefficient of a pair of coupled oscillators displays hysteresis as the coupling strength is varied. They define critical coupling strengths as the values where jumps occur and where the correlation coefficients are still equal to unity.

We perform similar simulations and evaluate both the correlation coefficient C_i^{12} and the average distance ΔX^{12} as follows. At each value of the coupling strength, we discard an initial transient period of 40 000 s and then evaluate C_i^{12} and ΔX^{12} according to Eqs. (4) and (5), respectively, from the time series for the next 60 000 s with data points taken approximately every second ($N\approx60\,000$). The last data point in one time series is used as the initial condition for a simulation with a new value of the coupling strength.

We choose one of three chaotic states determined by the flow rate k_o (see Fig. 1): (a) from a narrow chaotic window, with $k_o=6.52\times10^{-4}\ s^{-1}$, (b) from the middle of a wide chaotic window, with $k_o=7.24\times10^{-4}\ s^{-1}$ and (c) near the edge of the wide chaotic window in (b), with $k_o=7.19\times10^{-4}\ s^{-1}$. In Fig. 3 we show how our measures of synchronization display hysteresis for $k_o^{(1)}=k_o^{(2)}=7.19\times10^{-4}\ s^{-1}$. We observe that the synchronization and desynchronization processes occur gradually, without noticeable jumps, as the coupling is increased and decreased, respectively. Somewhat arbitrarily, we choose the value $\Delta X^{12}=1\times10^{-10}M$ to define the critical coupling strength $k_c^{\rm crit}$. In Table II we give, for our three chaotic states (a), (b), and (c), the calculated values of $k_c^{\rm crit}$ together with the ratio $\lambda_{\max}/k_c^{\rm crit}$, where $\lambda_{\max}$ is the maximal Lyapunov exponent in the uncoupled subsystem.

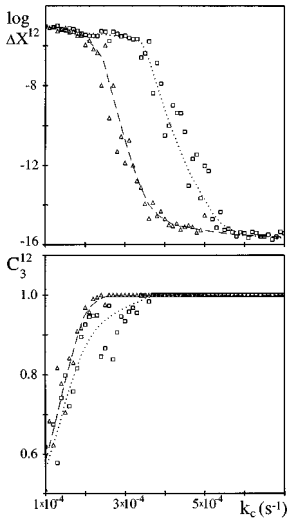

FIG. 3. Synchronization of two identical chaotic oscillators. Dependence of average distance ΔX^{12} and correlation coefficient C_3^{12} on coupling strength k_c for $k_o^{(1)}=k_o^{(2)}=7.19\times10^{-4}$ s^{-1}. Squares and dotted line show increasing coupling strength; triangles and dashed line show decreasing coupling strength.

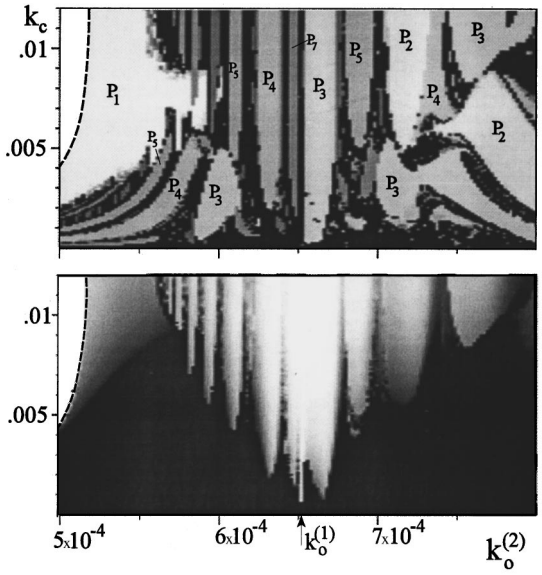

FIG. 4. Synchronization of nonidentical chaotic-chaotic and chaotic-periodic oscillators in the vicinity of identical oscillators. Reactor no. 1 is in chaotic state with fixed $k_o^{(1)}=6.52\times10^{-4}$ s^{-1}. Top frame displays dynamics in cell no. 1 with gray levels: white denotes the stable steady state, black signifies chaos, and all other gray levels show periodic regimes. The lighter the gray level the smaller the periodicity; P_i designates the periodicity of a periodic regime. Bottom frame displays values of correlation coefficients with gray levels. Black indicates domains with $C_3^{12}\leqslant0.9$ and white domains of complete synchronization ($C_3^{12}=1.0$). For $0.9<C_3^{12}<1$, lighter gray corresponds to higher correlation coefficient.

C. Dynamics of nonidentical chaotic oscillators

We have also investigated the behavior of coupled nonidentical chaotic oscillators as follows. We integrate Eqs. (2) for a fixed flow rate in reactor no. 1. The flow rate $k_o^{(2)}$ and the coupling strength k_c are first fixed at their minimum values, and then k_c is increased step by step. When k_c reaches a preset maximum value, the flow rate $k_o^{(2)}$ is increased while k_c is reset to its minimum value. The initial conditions are taken for subsequent simulations as the last data point of the previous simulation. The dynamics and the correlation coefficient are estimated from the stationary time series at each set of parameters. We define synchronized regimes in terms of the correlation coefficient for $[Ce^{4+}]$, $C_3^{12}>0.9$, and asynchronous regimes as those with $C_3^{12}<0.9$. Figure 4 displays the domains of synchronized and asynchronous regimes in the $k_c-k_o^{(2)}$ parameter plane with $k_o^{(1)}$ fixed at 6.52×10^{-4} s^{-1} and $k_o^{(2)}$ not very different from $k_o^{(1)}$. The structure of synchronized regimes resembles the Arnold tongues. Comparing the synchronized regions in the lower frame of Fig. 4 with the dynamical behavior summarized in the upper frame demonstrates that the domains of synchronized behavior coincide with domains of periodic behavior. Thus domains of periodic behavior for the coupled system of nonidentical oscillators are domains with higher correlation than domains of chaotic behavior. The only exception to this observation occurs in the chaotic window surrounding the region where the two flow rates are equal, so that the subsystems are identical.

In Fig. 5 we investigate a broader range of flow rates $k_o^{(2)}$, i.e., a more dissimilar pair of coupled reactors. The top and middle frames of Fig. 5 show the structure of the oscillatory regions in the two reactors. The conditions in reactor no. 1 correspond to chaotic behavior in an uncoupled subsystem. Depending upon the conditions in the second reactor and on the intensity of coupling, the chaotic oscillations may remain chaotic (synchronized or desynchronized), become periodic (either simple or complex), or the system may cease to oscillate.

The domains of periodic behavior are significantly larger than the domains of chaotic oscillation. The largest domains belong to the synchronized period-1 oscillations located to the left and right of the central part of the diagram. There are two other domains of period-1 behavior, which border on the regions in which the steady state is stable. Two large domains in the central part of the diagram correspond to frequency locking, one with ratio 1:2 and the other with ratio 2:3.

TABLE II. Critical coupling strength.[a]

$k_0[s^{-1}]$	λ_{max}	$\uparrow k_c^{crit}$	$\downarrow k_c^{crit}$	$\lambda_{max}/\uparrow k_c^{crit}$	$\lambda_{max}/\downarrow k_c^{crit}$
6.52×10^{-4}	$+2.02\times10^{-3}$	6.8×10^{-4}	6.0×10^{-4}	2.97	3.37
7.19×10^{-4}	$+1.14\times10^{-3}$	4.0×10^{-4}	2.9×10^{-4}	2.78	3.93
7.24×10^{-4}	$+3.34\times10^{-3}$	1.16×10^{-3}	9.6×10^{-4}	2.93	3.48

[a]$\uparrow k_c^{crit}$—critical value of k_c for increasing coupling; $\downarrow k_c^{crit}$—critical value of k_c for decreasing coupling.

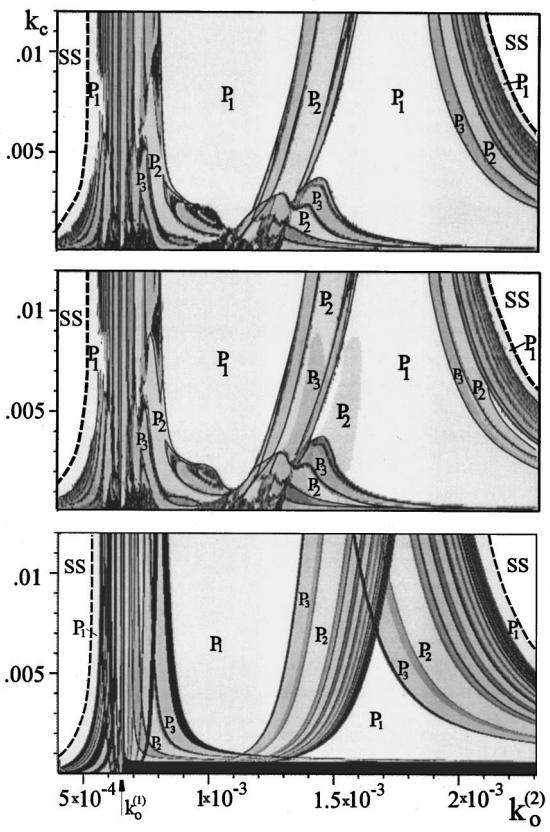

FIG. 5. Dynamics in a system of coupled chaotic oscillators. Top frame displays dynamics in reactor no. 1, middle frame the dynamics in reactor no. 2, bottom frame the prediction by simple model (see Sec. III D). Gray levels show periodicity of the oscillations. P_i designates domains with periodic oscillations of period i. SS is domain of stable steady state. Dashed line is Hopf bifurcation line, separating region of stable steady state and domain of oscillations. Parameters as in Fig. 4.

D. A simple model for predicting the dynamics of coupled systems

If we examine Figs. 1 and 5, we see that the dynamical bifurcation structure of the coupled oscillators resembles that of the uncoupled subsystem. This similarity of dynamical behavior increases with the coupling strength, which is, of course, to be expected, since in the limit of infinite coupling, the two subsystems must behave as a single, synchronized system. These observations encourage us to seek a simple model for predicting the dynamics of a coupled system primarily from the dynamical structure of the uncoupled subsystems.

We make the assumption that the most important effects of the coupling can be represented by changes in the effective values of the parameters. In our simulations, the only parameter that differs in the two reactors is the flow rate. We seek to evaluate the effective values of the flow rate, denoted as $k_{oe}^{(1)}$ and $k_{oe}^{(2)}$, starting from the hypothesis that the coupling acts to diminish the difference between parameters in a symmetric way according to

$$k_{oe}^{(i)} = k_o^{(i)} - \Delta k, \tag{6a}$$

$$k_{oe}^{(j)} = k_o^{(j)} + \Delta k, \tag{6b}$$

where $k_o^{(i)} > k_o^{(j)}$, $i,j = 1,2$, $i \neq j$, Δk denotes the apparent change of the flow rate due to coupling.

The dynamics of the coupled system is then predicted from the behavior of the uncoupled subsystems at the effective values of the flow rate. We assume that the coupled system will adopt the regime of higher periodicity. An example of this assumption is shown schematically in Fig. 6. When one effective parameter lies in a steady state regime, the dynamics is determined by the behavior of the other subsystem; if one regime is chaotic, then the coupled system should behave chaotically.

The key to quantifying our model is to establish how the apparent change in the flow rate Δk depends on the coupling strength k_c and on the difference between $k_o^{(1)}$ and $k_o^{(2)}$, which we take to be the two relevant quantities that determine Δk. We make the assumption that Δk depends linearly on the absolute value of the difference between parameters

$$\Delta k = f(k_c)|k_o^{(1)} - k_o^{(2)}|/2, \tag{7}$$

where $f(k_c) \in \langle 0,1 \rangle$. Clearly, $f(0) = 0$, and we make the reasonable assumption that f is a monotonically increasing function of k_c. At infinite coupling strength both oscillators behave as if they were identical ($f = 1$), and the maximal apparent change is $|k_o^{(1)} - k_o^{(2)}|/2$.

To determine $f(k_c)$ in detail, we make use of one piece of information about the coupled system, the primary Hopf bifurcation lines from the k_c vs $k_o^{(2)}$ bifurcation diagram as shown in Fig. 2. In effect, we assume that if we know, as a function of the coupling strength, the flow rate at which period-1 oscillation begins in the coupled system, we will be able to predict the onset of higher periodic and chaotic behavior in that system as well.

Our analysis is shown schematically in Fig. 7(a), where k_L and k_R are the lower and upper values, respectively, of the flow rate at the primary Hopf bifurcations in the uncoupled

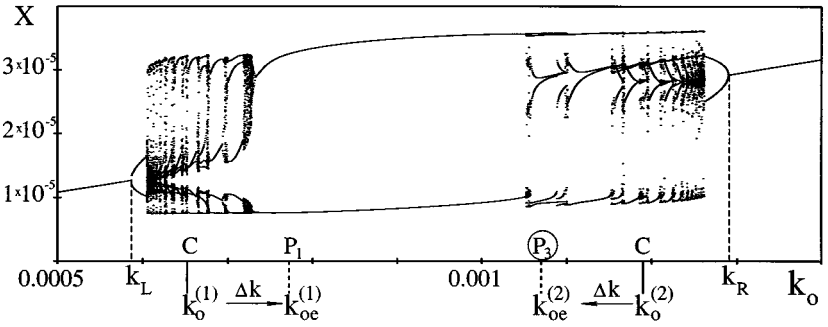

FIG. 6. Schematic prediction of dynamics of two nonidentical coupled oscillators from dynamics of subsystems. Prediction is based on assumption that coupling affects subsystem parameters so as to diminish the difference between them. At the chosen coupling strength, the corresponding dynamics for effective flow rate $k_{oe}^{(1)}$ is period-1 oscillation, while for $k_{oe}^{(2)}$ we have a period-3 oscillation. The coupled system is predicted to adopt the period-3 oscillation.

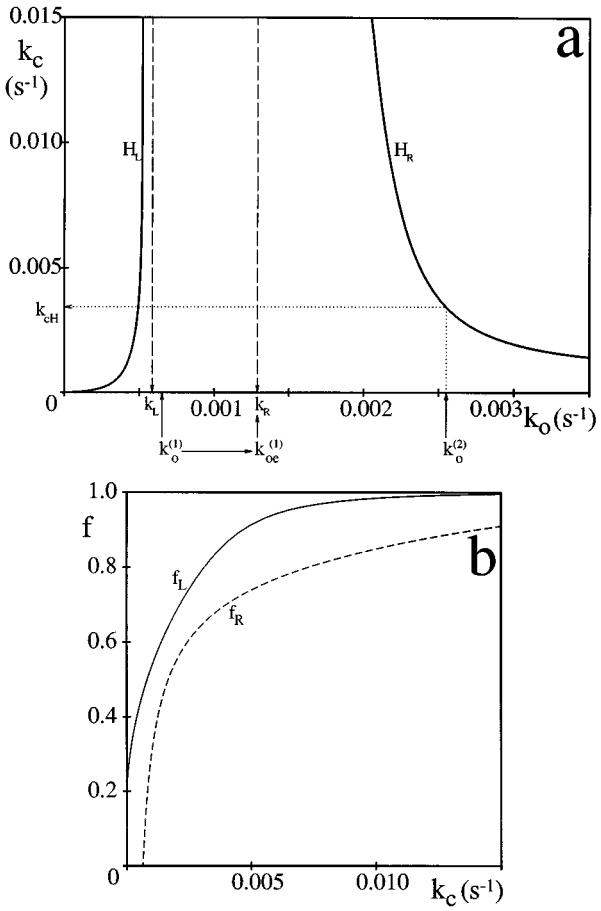

FIG. 7. Method of evaluating function $f(k_c)$ in Eq. (7) from Hopf bifurcation lines of coupled system (a) and results of evaluating $f(k_c)$ (b). Reactor no. 1 is in chaotic state with fixed $k_o^{(1)}=6.52\times10^{-4}$ s^{-1}. Effective value $k_{oe}^{(1)}$ becomes equal to k_R when the pair of values $(k_o^{(2)},k_c)$ lies on the Hopf line H_R, while the effective value $k_{oe}^{(2)}$ is larger than k_R. f_L: function obtained using points on left Hopf line H_L; f_R: function obtained using points on right Hopf line H_R.

system, and the solid lines H_L and H_R delineate the primary Hopf bifurcations in the coupled system when $k_o^{(1)}$ is fixed at the value indicated. First, consider the case when $k_o^{(2)}>k_o^{(1)}$ [Fig. 7(a)]. Since the $k_o^{(1)}$ that we have chosen lies between k_L and k_R, the system will oscillate for small values of k_c, because reactor no. 1 lies in the oscillatory parameter range. As we increase the coupling, $k_{oe}^{(1)}$ increases until, when $k_c=k_{cH}$, it reaches k_R. If the coupling is increased still further, both $k_{oe}^{(1)}$ and $k_{oe}^{(2)}$ will lie to the right of k_R, so that both effective flow rates will lie outside the oscillatory region and, according to our assumptions, the coupled system will no longer oscillate. The pair of values $(k_c,k_o^{(2)})$ thus lies along the Hopf bifurcation line [H_R in Fig. 7(a)] of the coupled system. The border of the oscillatory region in the coupled system is then associated with the equivalence of the Hopf bifurcation point value k_R of the uncoupled system with the effective value $k_{oe}^{(1)}$. At such a point, the apparent change of the flow rate Δk is

$$\Delta k=k_R-k_o^{(1)}. \tag{8}$$

Combining Eqs. (6), (7), and (8), we obtain

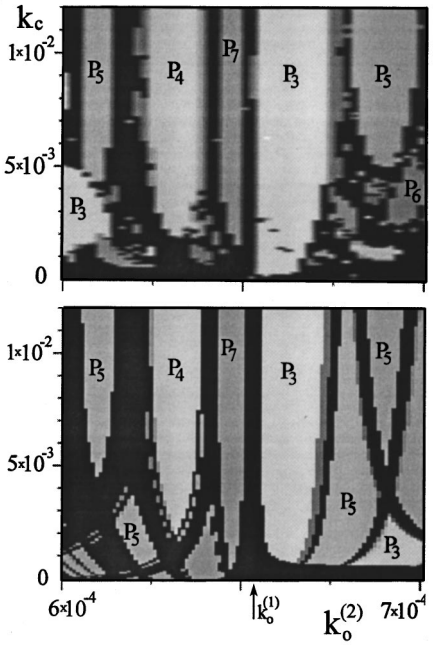

FIG. 8. Dynamics of coupled chaotic oscillators near identical conditions. Top frame displays results of direct simulations, bottom frame displays results predicted by simple model. Gray levels show periodicity of the oscillations. P_i designates domains of period-i oscillations. Black regions are chaotic. Parameters as in Fig. 4.

$$f(k_c)=2[k_R-k_o^{(1)}]/[k_o^{(2)}(k_c)-k_o^{(1)}]=f_R(k_c), \tag{9}$$

where, for the given fixed $k_o^{(1)}$, the dependence of $k_o^{(2)}$ on k_c is determined by the Hopf curve H_R. Similarly, when $k_o^{(1)}>k_o^{(2)}$, the effective value $k_{oe}^{(1)}$ coincides with k_L, while $k_{oe}^{(2)}<k_L$ for any pair $(k_c,k_o^{(2)})$ along the Hopf line H_L, and f is given by

$$f(k_c)=2[k_o^{(1)}-k_L]/[k_o^{(1)}-k_o^{(2)}(k_c)]=f_L(k_c). \tag{10}$$

The functions $f_R(k_c)$ and $f_L(k_c)$ are plotted in Fig. 7(b). If Eq. (7) were valid over the entire parameter range, the functions f_R and f_L would be identical. The discrepancy between the functions indicates the imperfection of the model. A simple modification consists of the following assignment for $f(k_c)$:

$$\begin{aligned} f&=f_L \quad \text{when } k_o^{(2)}<k_o^{(1)},\\ f&=f_R \quad \text{when } k_o^{(2)}>k_o^{(1)}. \end{aligned} \tag{11}$$

The dynamics predicted by the above model is displayed in the bottom frame of Fig. 5 and in Fig. 8. Figure 8 shows the dynamics in the vicinity of identical conditions $(k_o^{(1)}=k_o^{(2)})$, where the predictions of the model are in excellent agreement with the results of direct simulations. The largest discrepancies between the model predictions and direct integration occur at weak couplings $(k_c<1\times10^{-3}$ $s^{-1})$. Formulation of a reliable simple model at such coupling is a formidable task. The results predicted by this simple model appear to be in good qualitative agreement with direct simulation even for the wider range of parameter differences examined in Fig. 5. The major domains obtained by integration of the full set of equations are predicted by the simple model,

supporting our assumption that information about higher periodicities and chaos can be obtained from knowledge only of the behavior of the uncoupled systems and the primary Hopf bifurcation of the coupled system.

IV. DISCUSSION

The present investigation represents only a beginning step in the study of coupled chaotic chemical oscillators. Oscillator death in coupled chemical systems has been reported earlier for periodic oscillators [4,7,8,12], but to our knowledge there are no previous reports of oscillator death in mass coupled chaotic oscillators. Oscillator death in our model of the BZ reaction is not associated with a particular chaotic or periodic mode but, as Fig. 2 shows, it occurs in a range of $k_o^{(1)}$ and $k_o^{(2)}$ in which both periodic and chaotic oscillations are found in a single CSTR. Because of the symmetry of the coupled system, the region of oscillator death for $k_o^{(1)} > 1.26\times10^{-3}$ s^{-1} is complementary to a similar region for $k_o^{(1)} < 6.8\times10^{-4}$ s^{-1}.

Our direct simulations do not reveal the oscillator death that is predicted by the continuation method to occur inside the oscillatory region [see Figs. 2(iii) and 5]. The explanation for this failure is to be found in the subcriticality of the bifurcation and in the initial conditions. The domain of oscillator death is located inside the domain of synchronized period-1 oscillations. As noted above, the initial conditions of each simulation correspond to the final data point of the previous simulation. When we increase the coupling strength so as to enter the domain of oscillator death, the initial conditions always lie within the basin of attraction of the stable limit cycle. The stable steady state can be attained by perturbing this initial state to place the system within the steady state's basin of attraction.

One type of oscillator death has been explained for coupled identical oscillators as arising from an out-of-phase entrainment mode [8,16]. In such cases the chemical ''force'' that tends to ''push'' the two subsystems apart as they move out of phase around the limit cycle is balanced by the ''pull'' of the coupling. Our simulations reveal the presence of oscillator death in coupled chaotic oscillators, but only for specific nonidentical conditions. A similar type of oscillator death has been observed in two coupled Lorenz systems [43]. Although our model at the parameters studied does not give rise to the stable out-of-phase entrainment reported in Refs. [7] and [8], the oscillator death in our simulations can also be thought of as emerging from a balance between the coupling and the tendency toward out-of-phase entrainment. The balance can be destroyed by perturbation, after which the system begins to oscillate.

We have looked at identical oscillators in low flow rate chaos to study the synchronization and desynchronization of coupled chaos and to test the method of determining the maximum Lyapunov exponent from the critical coupling strength. Fujisaka and Yamada [17] derived a relation between the critical coupling strength and the maximum Lyapunov exponent

$$\lambda_{\max} = 2k_c^{\mathrm{crit}}. \tag{12}$$

Our values of the ratio $\lambda_{\max}/k_c^{\mathrm{crit}}$, summarized, in Table II support the existence of a relationship like Eq. (12), but they are not in good agreement as to the constant of proportionality. The exact value of $\lambda_{\max}/k_c^{\mathrm{crit}}$, of course, depends on the determination of the critical coupling strength, which for our data is somewhat arbitrary. A smaller choice for our synchronization criterion [e.g., $\Delta X^{12} = 1\times10^{-14}$ M, see Fig. 3(b)] would give a result closer to that of Eq. (12). Hauser and Schneider [32] and also Schuster, Martin, and Martienssen [44] obtained similar deviations from the theoretical value.

The model introduced here for predicting the behavior of coupled nonidentical systems has both strong and weak points. It provides fast preliminary prediction of the dynamical behavior of two coupled oscillators that differ only in one parameter. If the parameter difference is relatively small the model gives nearly quantitative agreement with the actual dynamics. The main disadvantage of the model is its weak prediction for small k_c and for large differences $|k_o^{(1)} - k_o^{(2)}|$. The model also fails to reveal the domains of oscillator death and frequency locking. Utilizing the model requires the existence of supercritical Hopf bifurcations at both low and high values of the parameter.

In addition to refining the model further and examining how the conclusions of the present study are affected by changes in the nature of the component subsystems, further studies are needed to explore the feasibility of extending our approach to systems that differ in more than one parameter and to systems consisting of three or more coupled subsystems.

ACKNOWLEDGMENTS

We gratefully acknowledge the support of the National Science Foundation Chemistry Division and the W. M. Keck Foundation.

[1] M. Marek and I. Stuchl, Biophys. Chem. **3**, 241 (1975).
[2] H. Fujii and Y. Sawada, J. Chem. Phys. **69**, 3830 (1978).
[3] I. Stuchl and M. Marek, J. Chem. Phys. **77**, 2956 (1982).
[4] K. Bar-Eli and S. Reuveni, J. Phys. Chem. **89**, 1329 (1985).
[5] M. F. Crowley and R. J. Field, J. Phys. Chem. **90**, 1907 (1986).
[6] M. Dolnik, E. Padušáková, and M. Marek, J. Phys. Chem. **91**, 4407 (1987).
[7] M. Dolnik and M. Marek, J. Phys. Chem. **92**, 2452 (1988).
[8] M. F. Crowley and I. R. Epstein, J. Phys. Chem. **93**, 2496 (1989).
[9] J. P. Laplante and T. Erneux, J. Phys. Chem. **96**, 4931 (1992).
[10] M. Dolnik and I. R. Epstein, J. Chem. Phys. **98**, 1149 (1993).
[11] J. Kosek and M. Marek, J. Phys. Chem. **97**, 120 (1993).
[12] K. Bar-Eli, J. Phys. Chem. **88**, 3616 (1984).
[13] I. Schreiber, M. Holodniok, M. Kubíček, and M. Marek, J. Stat. Phys. **43**, 489 (1986).
[14] C. G. Hocker and I. R. Epstein, J. Chem. Phys. **90**, 3071 (1989).
[15] K. Bar-Eli, J. Phys. Chem. **94**, 2368 (1990).
[16] I. R. Epstein, Commun. Mol. Cell. Biophys. **6**, 299 (1990).

[17] H. Fujisaka and T. Yamada, Prog. Theor. Phys. **69**, 32 (1983).
[18] H. Daido, Prog. Theor. Phys. **72**, 853 (1984); Prog. Theor Phys. Suppl. **79**, 75 (1984).
[19] K. Kaneko, Phys. Rev. Lett. **65**, 1391 (1990).
[20] A. Piskunov and P. Grassberger, J. Phys. A **24**, 4587 (1991).
[21] S. Sinha, D. Biswas, M. Azam, and S. V. Lawande, Phys. Rev. A **46**, 6242 (1992).
[22] H. Gang and Q. Zhilin, Phys. Rev. Lett. **72**, 68 (1994).
[23] T. Ushio, Phys. Lett. A **198**, 14 (1995).
[24] J. Losson, J. Milton, and M. C. Mackey, Physica D **81**, 177 (1995).
[25] N. F. Rulkov, M. M. Sushcnik, L. S. Tsimring, and H. D. I. Abarbanel, Phys. Rev. E **51**, 980 (1995).
[26] B. Röhricht, B. Wessely, J. Peinke, A. Mülbach, J. Parisi, and R. P. Huebener, Physica B **134**, 281 (1985).
[27] Y. Liu and J. R. Rios Leite, Phys. Lett. A **191**, 134 (1994).
[28] Y. Liu, P. C. de Oliveira, M. B. Danailov, and J. R. Rios Leite, Phys. Rev. A **50**, 3464 (1994).
[29] P. Ashwin, J. Buescu, and I. Stewart, Phys. Lett. A **193**, 126 (1994).
[30] J. Halloy, Y. X. Li, J. L. Martiel, B. Wuster, and A. Goldbeter, Phys. Lett. A **151**, 33 (1990).
[31] S. I. Doumbouya, A. F. Münster, C. J. Doona, and F. W. Schneider, J. Phys. Chem. **97**, 1025 (1993).
[32] M. J. B. Hauser and F. W. Schneider, J. Chem. Phys. **100**, 1058 (1994).
[33] B. P. Belousov, in *Sb. Ref. Radiats. Med.* (Medgiz, Moscow, 1958), p. 145; A. M. Zhabotinsky, Biofizika **9**, 306 (1964).
[34] R. A. Schmitz, K. R. Graziani, and J. L. Hudson, J. Chem. Phys. **67**, 3040 (1977).
[35] J. L. Hudson, M. Hart, and D. Marinko, J. Chem. Phys. **71**, 1601 (1979); J. L. Hudson and J. C. Mankin, J. Chem. Phys. **74**, 6171 (1981).
[36] L. Gÿorgyi and R. J. Field, Nature **355**, 808 (1992).
[37] L. Gÿorgyi and R. J. Field, J. Phys. Chem. **95**, 6594 (1991).
[38] F. W. Schneider and A. F. Münster, J. Phys. Chem. **95**, 2130 (1991).
[39] L. Gÿorgyi, R. J. Field, Z. Noszticzius, W. D. McCormick, and H. L. Swinney, J. Phys. Chem. **96**, 1228 (1992).
[40] G. B. Ermentrout and N. Kopell, SIAM (Soc. Ind. Appl. Math.) J. Appl. Math. **50**, 125 (1990).
[41] A. Wolf, J. B. Swift, H. L. Swinney, and J. A. Vastano, Physica D **16**, 285 (1985).
[42] M. Marek and I. Schreiber, in *Chaotic Behavior of Deterministic Dissipative Systems* (Cambridge University, Cambridge, England, 1991).
[43] A. Stefanski and T. Kapitaniak, Phys. Lett. A **210**, 279 (1996).
[44] H. G. Schuster, S. Martin, and W. Martienssen, Phys. Rev. A **33**, 3547 (1986).